Gene Ther. Author manuscript; available in PMC 2016 August 09.

Published in final edited form as:

Gene Ther. 2014 November ; 21(11): 967–974. doi:10.1038/gt.2014.77.

Overexpression of X-Linked Inhibitor of Apoptotic Protein (XIAP) Reduces Age-related Neuronal Degeneration in the Mouse Cochlea

Qingwei Ruan[a,b,*], **Shan Zeng**[a,*], **Aiguo Liu**[c,*], **Zhengnong Chen**[a], **Zhuowei Yu**[b], **Ruxin Zhang**[b], **jingchun He**[a], **Manohar Bance**[d,e], **George Robertson**[d,f], **Shankai Yin**[a,#], and **Jian Wang**[a,d,g,#]

[a]Dept. and Research Institute of Otolaryngology, the Sixth Affiliated Hospital of Shanghai Jiaotong University, 600 Yi Shan Road, Shanghai 200233, P.R. China

[b]Research Center of Aging and Medicine, Shanghai Key Laboratory of Clinical Geriatrics, Huadong Hospital, Shanghai Medical College, Fudan University, Shanghai 200040, China

[c]Dept. of Otolaryngology, Tongji Hospital, Tongji medical college, Huazhong University of Science & Technology, 1095 Jie Fang Avenue, Wuhan 430030, P.R. China

[d]Division of Otolaryngology, Dept. of Surgery, Dalhousie University, Halifax, Nova Scotia, Canada

[e]Dept. of Anatomy and Neurobiology, Dalhousie University, Halifax, Nova Scotia, Canada

[f]Dept. of Psychiatry and Pharmacology, Dalhousie University, Halifax, Nova Scotia, Canada

[g]School of Human Communication Disorders, Dalhousie University, 1256 Barrington St., Halifax, Canada, B3J1Y6

Abstract

Previously, we showed that age-related hearing loss (AHL) was delayed in C57BL6 mice overexpressing X-Linked Inhibitor of Apoptotic Protein (XIAP), and the delayed AHL was associated with attenuated hair cell (HC) loss in XIAP-overexpressing mice. Similar to other reports, the HC loss in aged mice was restricted to the basal turn in this previous study, and occurred slightly at the apical end of the cochlea, showing considerably less spread than the frequency region of hearing loss. In the present study, we examined whether and how AHL is related to the degeneration of neuronal innervation of the cochlea and if the overexpression of XIAP exerts a protective effect against age-related degeneration in both afferent and efferent cochlear neurites. In contrast to HC loss, degeneration of both afferent and efferent neurites spread to the middle turns of the cochlea. Moreover, XIAP-overexpressing mice lost fewer HC afferent

[#]Corresponding authors: Jian Wang, Ph.D at SHCD of Dalhousie University, 1256 Barrington St. Halifax, Nova Scotia, Canada. B3J1Y6 Tel: 1-902-4945149 Fax: 1-902-4945151 Jian.Wang@dal.ca and Shankai Yin, PhD, MD at The Sixth People's Hospital, 600 Yi Shan Road, Shanghai 200233, P.R. China Tel: +011-86-21-24058926 Fax: +011-86-21-64834143 yinshankai@china.com.

[*]These authors contributed equally

Competing interest statement

The authors declare that no competing interests exist.

Supplementary information is available on the *Gene Therapy* website.

dendrites and efferent axons, as well as fewer spiral ganglion neurons (SGNs) between 3– 14 months of age in comparison to wild-type littermates. The results suggest that age-related degeneration of cochlear neurites may be independent of HC loss. Further, the inhibition of apoptosis by XIAP appears to reduce degeneration of both afferent and efferent cochlear neurites.

Keywords

Presbycusis; cochlear neurites degeneration; X-Linked Inhibitor of Apoptotic Protein

Introduction

Age-related hearing loss (AHL), or presbycusis, is associated with pathological findings in various cellular and structural components of the cochlea, including hair cells (HCs) [1,2], spiral ganglion neurons (SGNs) [3], the spiral ligament, spiral limbus, and stria vascularis [4,5]. However, the relative contributions of these cellular and structural pathologies to the development of presbycusis remain unclear. Destruction of HCs, especially the outer hair cells (OHCs), is considered to be a major contributor to AHL, because of the concordance between the frequency spectrum of hearing loss and the regions of HC degeneration within the cochlea found in mouse models [2,4]. However, HC loss cannot always explain the hearing loss exhibited, because HC loss may not occur in some regions where hearing loss is manifest [4,6]. This suggests that other pathological events are involved as precursors to HC death, or as alternate causes of hearing loss. In particular, we were interested in the cochlear neural elements. Degeneration of SGNs and/or their peripheral processes in response to aging has been found to be more severe and widespread than HC loss in several animal models [7 – 10]. This suggests that SGN degeneration may play an important role in the development of AHL.

Although the precise mechanisms responsible for age-related cell death in the cochlea remain unclear, apoptosis is thought to play a critical role in this process [11 – 16]. During presbycusis, apoptosis is activated through the intrinsic cell death pathway by the excessive production of free radicals in association with oxidative stress [11,13,16,17,18,19,20]. The most potent member of the Inhibitor of Apoptosis (IAP) family, X-Linked IAP (XIAP), blocks apoptosis initiated by either the intrinsic or extrinsic cell death pathways by inhibiting caspase-3, the final component of these pathways [21 – 25].

Aged C57BL/6J mice show premature AHL and display pathological changes in the auditory system indicative of AHL [26,27]. We reported previously that the development of presbycusis is delayed in transgenic (TG) C57BL/6J mice overexpressing XIAP under control of the ubiquitin promoter (ubXIAP) compared to wild-type (WT) littermates [6]. TG ubXIAP mice were also more resistant to noise-induced hearing loss than their wild-type littermates [28]. In both studies, HC loss was limited to the basal region of the cochlea responsive to sound frequencies above 10 kHz. Correspondingly, the HC loss protection in TG mice was seen only in the basal end of the cochlea. However, the functional changes and protection as demonstrated by the hearing threshold changes in both WT and TG mice

extended to the lower frequencies [6,28]. These findings suggest that XIAP preserves hearing function by protecting components of the cochlea other than the HCs.

In the present study, we revisited the protective effects of XIAP overexpression against presbycusis in TG mice, focusing on the neural elements in the cochlea. Cochlear neurites consist of two parts: afferent neurites serve as an ascending pathway for information from HCs to auditory brain areas via the SGNs in Rosenthal's canal in the cochlear modiolus, while efferent neurites comprise a descending pathway from the brain, particularly the lower brainstem, to cochlear HCs. Specific staining for two types of SGNs and their dendrites as well as the efferent axons was performed in this study in combination with sectioning techniques to differentiate and quantify the afferent dendrites and efferent axons. The aims of the present study were twofold: (1) to determine whether overexpression of XIAP in TG mice decreases age-related degeneration of cochlear neurites, and (2) to examine how the neuronal degeneration that develops with aging in this species is related to hearing loss and HC loss.

Results

XIAP overexpression delays the development of AHL

The thresholds of auditory brainstem responses (ABR) were measured at 3, 6, and 14 months of age in all animals until they reached their individual end points. Confirming the findings of our previous study [6], overexpression of XIAP resulted in a significant delay in the development of AHL in TG ubXIAP mice in comparison with WT controls. This delay of AHL in the TG group was already evident by 3 months of age: 5 – 10 dB lower ABR thresholds at frequencies above 8 kHz (Supplementary Fig. 1) for the TG group. The difference between the TG and WT groups was greater at 14 months (10 – 20 dB above 8 kHz, Supplementary Fig. 1). Similar to our previous findings, it was clear that the protection of hearing by XIAP overexpression was more effective in the high-frequency region (Supplementary Fig. 1). To further characterize the differences between the TG and WT groups in ABR thresholds across different frequency regions, we calculated the averaged thresholds for both low-frequency (2 – 8 kHz) and high-frequency (16 – 64 kHz) areas. Supplementary Fig. 2 shows the changes in frequency-averaged ABR thresholds as a function of age. It is clear that the high-frequency average in the TG group was slightly lower than that in the WT group at 3 months of age, and the advantage in the TG group increased at older ages (6 and 14 months).

XIAP reduces the losses of the two types of SGN

In the neuronal structures, age-related degeneration was seen in the reduction of both afferent dendrite and efferent axon counts as well as in the two types of SGN. Figure 1 shows representative cross-sections of Rosenthal's canal with triple staining with tetramethylrhodamine-conjugated dextran (TMRD) (red) for type I SGNs, peripherin (green) for type II SGNs, and 4′,6-diamidino-2-phenylindole (DAPI) for cellular nuclei. The age-related changes in SGN survival are summarized in Fig. 2, which shows the average numbers of SGNs in each section crossing Rosenthal's canal in the M5 segments (approximately 8 – 16 kHz, see Methods section for details regarding location). The data in

Fig. 2 were obtained from seven animals at each time point. Clear age-related reductions in the numbers of both types of SGNs were seen, with less of an effect in the TG group. Two-way ANOVAs were performed to analyze the degeneration in type I and II SGNs. For type I SGNs, significant effects were seen for both factors of genotype ($F_{1, 36} = 19.698$, $P < 0.001$ for less SGN degeneration in the TG group) and age ($F_{2, 36} = 55.863$, $P < 0.01$), as well as the interaction between the two factors ($F_{2, 41} = 5.282$, $P = 0.01$). The significance of the interaction was further supported by pairwise comparisons, which showed that within the factor of age, the between-group difference was not significant at 3 months of age but significant at 6 and 14 months ($t_{12} = 2.562$, $P = 0.015$ and $t_{12} = 4.861$, $P < 0.001$, respectively, for 6 and 14 months of age, Holm–Sidak method). The age-related increases in the differences of type I SGN degeneration were quantitatively demonstrated by the increase in effect size from r = 0.4667 at 6 months to 0.9321 at 14 months.

For type II SGNs, significant effects were seen for genotype ($F_{1,36} = 9.116$, $P = 0.005$) and age ($F_{2,36} = 13.374$, $P < 0.001$) but not for their interaction ($F_{2, 41} = 0.128$, $P = 0.88$). Although the between-group difference appeared larger at the later age as compared with the change in type I SGNs (Fig. 2), the effect size for the difference was found to be increased from r = 0.2973 at 3 months of age to 0.4167 and 0.5989 at 6 and 14 months, respectively. Again, pairwise comparisons showed that within the factor of age, the between-group difference began to be significant at 3 months of age and remained so toward 14 months ($t_{12} = 2.505$, $P = 0.0172$ at 3 months, Holm–Sidak method).

XIAP reduces the age-related degeneration of both afferent and efferent neurites

XIAP also reduced the degeneration of afferent dendrites and efferent axons. The degeneration of both afferents and efferents was observed at different sites from under the HCs to the modiolus. We could not distinguish between type I afferent dendrites and lateral olivocochlear (LOC) efferent axons under inner hair cells (IHCs) because anti-choline acetyltransferase (ChAT) antibody did not work well in whole-mount basilar membrane (BM) preparations. However, the total terminals of both LOC efferent axons and type I afferent dendrites (shown as red dots under IHCs) was obviously less at 3 months of age in WT mice than in the TG group (Supplementary Fig. 3). The obvious between-group difference in degeneration of terminals to OHCs was also seen at 3 months of age by TMRD staining (Supplementary Fig. 3). We could not differentiate the type II afferent dendrites from medial olivocochlear (MOC) axons under OHCs because anti-peripherin antibody did not work well in whole-mount basilar membrane preparations.

Anti-ChAT antibody worked well in cross-sections of habenula perforata (HP). The top panel of Figure 3 shows the orientation of sections across HP openings and the area that was used for counting of dendrite/axon numbers. The number of dendrites/axons was counted in cross-sections perpendicular to the HP. We counted the total number of dendrites/axons in a section in the M5 segment of BM with the same frequency range for the count of SGNs to cover 1 unit length (approximately 4 HPs). The lower 3 panels of Figure 3 show representative immunostaining images of HP cross-sections. The samples were double stained with TMRD in combination with either anti-peripherin or anti-ChAT antibody to count two types of afferent dendrites and efferent axons separately.

Figure 4 shows statistical data for the changes in the number of dendrites/axons counted in HP cross-sections as a function of age. An overall decrease was seen for all three types of dendrite/axon, but more survived in the TG groups at each time point for every type of dendrite/axon. Two-way ANOVA confirmed significant effects of genotype ($F_{1,18} = 655.89$, $P < 0.001$), age ($F_{2,18} = 721.99$, $P < 0.001$), and their interaction ($F_{2, 23} = 62.45$, $P < 0.001$) for type I afferent dendrite degeneration. Post hoc tests for pairwise comparisons (Holm–Sidak method) showed significant differences between genotype groups at all time points ($P < 0.001$). Similar effects of genotype and age were seen on both efferent axons ($F_{1, 18} = 235.91$, $P < 0.001$; $F_{2, 18} = 246.32$, $P < 0.001$) and type II afferent dendrites ($F_{1, 18} = 104.88$, $P < 0.001$; $F_{2, 18} = 135.74$, $P < 0.001$). A greater loss of cochlear neurites was seen in the WT group than the TG group as early as 3 months of age. Interestingly, this effect was seen earlier than that for SGN changes. Asterisks indicate significance of pairwise comparisons within the factor of age between the two groups in Fig. 4.

XIAP reduces the degeneration of cochlear neural structures by inhibiting apoptosis

Apoptosis was also examined by TUNEL staining in the M5 segment of the basilar membrane and corresponding region of Rosenthal's canal. XIAP overexpression decreased the apoptosis of various types of cochlear cell. Apoptosis was not evident in either the WT or TG group at 3 months of age (Fig. 5A and B), but was clearly seen at 6 months of age in both supporting cells and OHCs (Fig. 5C) as well as in SGNs (Fig. 5E) in WT mice, but not in TG mice (Fig. 5D and F).

Discussion

The major findings of the present study were as follows. 1) C57 mice showed rapid degeneration with aging in both efferent and afferent neurites. The degeneration of cochlear neural structures reported in the present study appeared to be much more severe than the HC loss in our previous study [6]. 2) Neuronal degeneration in the cochlea can be significantly reduced by overexpression of XIAP.

Previous studies by other groups indicated that loss of both IHCs and OHCs with aging spreads from the two ends toward the middle part of the cochlea, with greater losses at the basal end compared to the apical part, and greater loss of OHCs than IHCs [2,4]. Comparison of the data among the studies cited above suggested that in this strain of mice, the loss of IHCs in the middle turn (8 – 32 kHz) was trivial at the ages of 6 and 14 months (< 5% and 25%, respectively). The reported OHC loss in this region ranged from less than 10% to 60% [2,4,6]. No HC loss was seen in the region of M5 (8 – 16 kHz) at 3 months of age (Fig. 5). However, the losses of type I dendrites at these ages in M5 observed in this study were 36.35% (3 months), 61.03% (6 months), and 74.89% (14 months), which were considerably greater than the corresponding IHC losses. The losses of type II dendrites were 11.68% (3 months), 42.49% (6 months), and 58.27% (14 months), which were also greater than the corresponding OHC losses at each time point in this region. Although there were significantly fewer type I and type II fibers at 3 months of age, this difference may not have been due to aging per se but rather to increased survival of the two types of neurons during development in TG mice. Our data also indicated that the dendrite losses preceded both type

I and type II SGN losses, consistent with a previous report in C57BL/6J mice (10). The difference between dendritic loss and SGN loss was less with advancing age (Figs. 1 – 2 and 3 – 4), likely due to the later degenerative death of SGNs.

As there was no significant IHC loss even at 14 months of age in this strain of mice, the degeneration of type I afferent fibers and SGNs cannot be simply considered as secondary to the loss of IHCs. As it started prior to the loss of SGNs, the degeneration of afferent dendrites may originate from the synapses between IHCs and SGNs, rather than from IHCs (Supplementary Fig. 3). The loss of the synapses and degeneration of afferent dendrites would result in interruption of the supply of neurotrophic factors, such as neurotrophin-3 (NT3), which are released from HCs and supporting cells and are critical for the survival of SGNs [29,30]. Therefore, the damage to the synapses may have been the initial locus for age-related SGN degeneration. However, it is not yet clear if SGN degeneration is entirely independent of IHCs. It is possible that the ability of IHCs to release trophic factors may deteriorate with age well before their death. If this is the case, the damage and disconnection between IHCs and SGNs may be due to malfunction of IHCs. Such degeneration could still be considered secondary to IHC malfunction, but not necessarily the death of IHCs and supporting cells. This could also explain the reported loss of SGNs after noise insult, which does not cause IHC loss or changes in hearing thresholds [29]. To our knowledge, little information is currently available regarding how the neurotrophic support for SGNs derived from HCs and supporting cells changes with aging. Furthermore, if any particular IHC loses its function for trophic support, all SGNs that innervate this IHC should be equally impacted. Therefore, degeneration of the terminals should be clustered to individual IHCs. Further studies are required to determine whether this is indeed the case.

Although neuronal degeneration develops ahead of HC death and corresponds better to the frequency region of functional hearing loss, it is not clear whether SGN loss causes the hearing losses indicated by threshold elevations at those frequencies. At present, we do not have adequate evidence of a strong correlation between SGN loss and threshold elevation during aging. First, we did not examine the dynamic process of cochlear neural degeneration and hearing threshold elevation, and investigated only discontinuous time samples. Second, even if the time course of SGN loss follows that of threshold elevation, we cannot simply attribute the hearing loss to the loss of SGNs, because a large proportion of SGNs can be killed without changes in the hearing threshold [29,31].

Our previous work demonstrated that XIAP overexpression in TG mice reduced age-related HC loss and preserved hearing [6]. Consistent with these findings, the loss of cochlear neural structures (afferent dendrites, two types of SGNs, and efferent axons) in transgenic mice was also less than those in wild-type mice. These observations indicated that XIAP prevented the loss of cochlear neural structures by suppressing cellular apoptosis during aging in many cell types.

Apoptosis is involved in cell death in the aged cochlea [11,15,16,19,20]. The presence of DNA fragmentation is seen predominantly in the OHCs and SGNs, and sporadically in supporting cells, IHCs, stria vascularis, spiral ligament, and in Reissner’s membrane in C57BL/6J mice [3,5,19,26,32]. In the aging cochlea, apoptosis of SGNs may be initiated by

the reduced supply of neurotrophic factors from the IHCs and supporting cells. As we reported previously, the transgene caused a ~50% increase in XIAP levels in the cochlea [6], and this increase in XIAP appears to be beneficial for the survival of both HCs and SGNs (Fig. 5).

The mechanisms responsible for degeneration of type II afferent dendrites and efferent axons are not yet clear. The dendrite terminals of type II SGNs and MOC axons make direct contact with more than 10 OHCs via reciprocal synapses [33], and OHC loss may therefore be directly responsible for the loss of type II dendrites, type II SGNs, and MOC axons. However, as yet there is no clear evidence that the survival of either type II SGNs or efferent neurons relies on the release of neurotrophins from OHCs. Moreover, it is not clear whether damage to the efferent neurites spreads from the organ of Corti to the bodies of neurons in the cochlear nuclei.

In summary, we have shown in a mouse model of AHL that: (1) degeneration of both afferent and efferent neurites to cochlear hair cells precedes HC loss; (2) the SGN degeneration appeared to spread from their fibers to their bodies; and (3) XIAP overexpression significantly delayed the neural degeneration process associated with aging. Further studies are needed to identify the mechanisms underlying SGN degeneration starting from the synapses.

Methods

Subject grouping and schedule

All procedures were approved by the Animal Ethics Committee of Shanghai Jiao Tong University, Shanghai, China. The origins of the transgenic (TG) and wild-type (WT) mice used in this study were described previously [6]. The TG mice were inbred from the transgenic founders. To obtain wild-type littermates for this experiment, ubXIAP animals were crossed with WT C57BL/6J mice. The mouse genotype with respect to XIAP was determined by PCR targeting the 6-Myc tag in the transgene. The Myc-XIAP C57 TG mice and WT littermates were bred and aged in the animal care facility at Shanghai Jiao Tong University.

A total of 84 mice (42 in WT and WT, respectively) were used in this experiment, and all underwent otoscopic examination to exclude any abnormalities in the outer or middle ear. We lost three animals in each group due to infections in the middle ear or accidental death by anesthesia. The data of hearing and cochlear morphology were collected at three ages: 3, 6, and 14 months (11 animals at each time point, making a subtotal of $11 \times 3 \times 2 = 66$). Of the 11 animals, 7 were used for analysis of SGNs and 4 for analysis of afferent dendrites and efferent axons. Six animals in each group were used for observation of apoptosis at both 3 and 6 months of ages (three at each time point, total = 12).

ABR measurement

ABRs were recorded from the animals under anesthesia with a ketamine–xylazine mixture (60 – 80 mg/kg + 10 mg/kg, i.p.). The animal was kept warm with a thermostatic heating pad. Signal generation and ABR acquisition were achieved using Tucker-Davis hardware

and BioSig software (TDT system III; Tucker-Davis Technologies, Alachua, FL). The stimuli consisted of tone bursts of 2, 4, 8, 16, 32, 48, and 64 kHz, with a duration of 10 ms and rise/fall of 1 ms (Blackman window). The signals were generated digitally and delivered to the animals through an electrostatic speaker (ES1; Tucker-Davis Technologies), which has a flat frequency response from 2 to 70 kHz. The speaker was placed 10 cm above the animal's head. The sound level was calibrated using a ¼-inch condenser microphone (Model 4349; Brüel & Kjær, Nærum, Denmark), which was placed at a position that would be occupied in experiments by the animal's head. The ABR was obtained using a stimulation rate of 21.1/s, and 1000 times averaging. The evoked responses were recorded by subdermal electrodes and band-pass filtered between 100 and 3000 Hz before amplification. At each frequency, the ABR was tested in a descending sequence from 90 dB sound pressure level (SPL) in steps of 5 – 10 dB until the threshold for a repeatable response was reached. If the evoked response was not detected at the highest sound presentation level (90 dB SPL) at any given frequency, the threshold at this frequency was labeled as 100 dB SPL. The ABR threshold was read out by an analyzer blinded to the age and genotype information of the animals.

Neuronal tracer application

Previous studies indicated that the neuronal tracer tetramethylrhodamine-conjugated dextran (TMRD) labels both cochlear efferent axons and type I (but not type II) afferent dendrites [34 –39]. Our method for applying TMRD was similar to that described previously [40]. Briefly, the animals were sacrificed by an overdose of sodium pentobarbital. The internal auditory meatus was exposed. A small piece of TMRD crystal was placed on the cochlear nerve bundle at the entrance of the internal auditory meatus for 20 min at 20°C. The excess dye crystal was removed by rinsing with Dulbecco's modified Eagle's medium (DMEM). The cochleae were harvested and a small hole was made at the apex for cochlear perfusion with the above medium. The cochleae were then incubated at 37°C for 3 h in DMEM supplemented with NT-3 (10 μg/mL), BDNF (30 μg/mL) (both from R&D Systems, Boston, MA) to prevent degeneration of SGN and neural dendrites and axons. After incubation, the cochleae were perfused with 4% paraformaldehyde in 0.1 M phosphate buffer (pH 7.4) and post-fixed with the same solution overnight at room temperature.

Immunostaining

After fixation, the TMRD-labeled cochleae were decalcified in a dark room with 150 mM EDTA for 4 d. The cochleae were dissected into lower and upper segments. Care was taken to preserve the HP and Rosenthal's canal. The spiral ligament, Reissners' membrane, and the tectorial membrane were removed and the samples were further decalcified with 150 mM EDTA for 8 h. The basilar membrane was divided into 13 segments, each ~0.4 mm in length and labeled as B1 – 4 for the basal turns, M1 – 5 for the middle turns, and A1 – 4 for the apical turns, respectively. In this study, neuronal degeneration was examined focusing on the M5 segment, roughly corresponding to the frequency range from 8 to 16 kHz.

To count afferent and efferent neurites in the HP openings, the whole-mount BM specimens were then dissected and all samples were embedded in TissueTek OCT compound (Sakura Finetechnical Co. Ltd., Tokyo, Japan), frozen in liquid nitrogen, and cut into serial sections

vertically across the HP openings at a thickness of 4 μm with a cryostat (Leica, Wetzlar, Germany). To count SGNs, the whole mount BM specimens were sectioned parallel to the HP opening to obtain cross-sectional images of Rosenthal's canal. Some cochleae were used for cochlear mid-modiolar sections. These cochleae were embedded in TissueTek OCT, frozen, and cut into serial sections parallel to the modiolus at a thickness of 8 μm. The cross-sections were incubated at 4°C for 1 h in blocking/permeabilizing solution containing 1% (w/v) bovine serum albumin (BSA), 5% heat-inactivated goat serum, and 1% Triton X-100 in 0.1 M PBS, and then incubated at 4°C overnight in a solution containing one of the primary antibodies raised in rabbits against peripherin (ab4666, at a dilution of 1:800) and ChAT (ab70129, at a dilution of 1:200; Abcam, Cambridge, UK). For signal detection, isothiocyanate-conjugated goat anti-rabbit IgG (KC-RB-095, at a dilution of 1:200) was applied at room temperature for 3 h (Kangchen Biotechnology, Shanghai, China). Peripherin is a 57-kDa type III intermediate filament protein specific to type II SGNs and dendrites [41 – 44].

TUNEL labeling

Apoptosis was evaluated by TUNEL labeling with a solution containing terminal deoxynucleotidyl transferase and TUNEL (Roche Molecular Biochemicals, Indianapolis, IN). After two washes with PBS, 50 μL of TUNEL reaction mixture were added to each sample. Negative controls were prepared using 50 μL of the control solution (without terminal deoxynucleotidyl transferase) in place of the TUNEL reaction mixture. The samples were incubated at 37°C for 60 min, and the reactions were stopped by washing three times with PBS. Cell nuclei of the samples were then stained with DAPI.

Image acquisition and data analysis

The images were obtained at 200× magnification with a regular optical microscope, a fluorescence microscope (Nikon, Tokyo, Japan), or a confocal microscope (ND2; Nikon). When using the confocal microscope, the maximum intensity of the projections generated from the optical section stacks was used to resolve labeled nerve fibers in the whole mount BM specimens or in the sectioned samples. Laser power, gain, and black level were carefully modulated between channels. These parameters were kept constant for all samples. The group identity was encoded so that all microscopy and computer analyses were performed in a blinded manner. For the dendrite/axon counts in the cross-sections of the HP, differentiation between afferent dendrites and efferent axons was based upon the following characteristics: The efferent axons were indicated by positive staining for ChAT, and type I afferent fibers were indicated by positive staining for TMRD without complete overlap with ChAT staining. Double-positive staining for both TMRD and ChAT suggested a type I fiber running together with an efferent axon. Type II afferent dendrites were indicated by positive staining with anti-peripherin antibody. As the border of each individual HP opening was not always clear, we did not calculate the number of dendrites/axons in each individual HP opening. Instead, we counted the dendrites/axons over a unit distance of 0.13 mm that covered approximately four consecutive HPs.

The type I SGNs were positive for TMRD staining, and so were distinguished from the type II neurons, which were positive for peripherin. In sections through Rosenthal's canal, the

two types of SGN were counted under a 20× visual field using the ImageJ software (NIH, Bethesda, MD). The SGN was counted in every fifth slice in the serial cross-sections of Rosenthal's canal in the M5 segment and averaged from three slices over a unit distance of 0.13 mm along the canal. The SNG count was expressed as the average number of SGNs in a unit area, which is the cross-sectional area of Rosenthal's canal. Two-way ANOVA was performed against the factors of genotype (TG vs. WT) and survival time to evaluate differences in the numbers of afferent dendrites, efferent axons, and SGNs. In all analyses, $P < 0.05$ was taken to indicate statistical significance. Post hoc tests were performed for the factors that showed significance in ANOVA. All data are presented as means ± SD in this paper.

Supplementary Material

Refer to Web version on PubMed Central for supplementary material.

Acknowledgments

This study was supported by a grant-in-aid for Scientific Research from Shanghai Municipal Health Bureau (No. 2011-4144), the State Key Development Program for Basic Research of China (Grant no. 2011CB504503 and no. 2012CB967903), the National Science Foundation for Distinguished Young Scholars of China (Grant no. 30925035), and the Canadian Institute of Health Research (MOP79452).

References

1. Garfinkle TJ, Saunders JC. Morphology of inner hair cell stereocilia in C57BL/6J mice as studied by scanning electron microscopy. Otolaryngology - Head & Neck Surgery. 1983; 91(4):421–426. [PubMed: 6415592]
2. Spongr VP, Flood DG, Frisina RD, Salvi RJ. Quantitative measure of hair cell loss in CBA and C57BL/6 mice throughout their life spans. J Acoust Soc Am. 1997; 101:3546–3553. [PubMed: 9193043]
3. White JA, Burgess BJ, Hall RD, Nadol JB. Pattern of degeneration of the spiral ganglion cell and its processes in the C57BL/6J mouse. Hear Res. 2000; 141(1–2):12–18. [PubMed: 10713491]
4. Hequembourg S, Liberman MC. Spiral ligament pathology: a major aspect of age-related cochlear degeneration in C57BL/6 mice. J Assoc Res Otolaryngol. 2001; 2(2):118–129. [PubMed: 11550522]
5. Shnerson A, Devigne C, Pujol R. Age-related changes in the C57BL/6J mouse cochlea. II. Ultrastructural findings. Brain Res. 1981; 254(1):77–88. [PubMed: 7272774]
6. Wang J, Menchenton T, Yin S, Yu Z, Bance M, Morris DP, et al. Over-expression of X-linked inhibitor of apoptosis protein slows presbycusis in C57BL/6J mice. Neurobiol Aging. 2010; 31(7): 1238–1249. [PubMed: 18755525]
7. Felder E, Schrott-Fischer A. Quantitative evaluation of myelinated nerve fibres and hair cells in cochleae of humans with age-related high-tone hearing loss. Hear Res. 1995; 91(1–2):19–32. [PubMed: 8647720]
8. Keithley EM, Ryan AF, Woolf NK. Spiral ganglion cell density in young and old gerbils. Hearing Research. 1989; 38(1–2):125–133. [PubMed: 2708154]
9. Ryals BM, Eyck BT, Westbrook EW. Ganglion cell loss continues during hair cell regeneration. Hearing Research. 1989; 43:81–90. [PubMed: 2613569]
10. Stamataki S, Francis HW, Lehar M, May BJ, Ryugo DK. Synaptic alterations at inner hair cells precede spiral ganglion cell loss in aging C57BL/6J mice. Hear Res. 2006; 221(1–2):104–118. [PubMed: 17005343]

11. Alam SA, Oshima T, Suzuki M, Kawase T, Takasaka T, Ikeda K. The expression of apoptosis-related proteins at the aged cochlea of Mongolian gerbils. Laryngoscope. 2001; 111(3):528–534. [PubMed: 11224787]
12. Iwai H, Lee S, Inaba M, Sugiura K, Tomoda K, Yamashita T, et al. Prevention of accelerated presbycusis by bone marrow transplantation in senescence-accelerated mice. Bone Marrow Transplant. 2001; 28(4):323–328. [PubMed: 11571502]
13. Pickles JO. Mutation in mitochondrial DNA as a cause of presbyacusis. Audiol Neurootol. 2004; 9(1):23–33. [PubMed: 14676471]
14. Spicer SS, Schulte BA. Spiral ligament pathology in quiet-aged gerbils. Hear Res. 2002; 172(1–2): 172–185. [PubMed: 12361880]
15. Tadros SF, D'Souza M, Zhu X, Frisina RD. Apoptosis-related genes change their expression with age and hearing loss in the mouse cochlea. Apoptosis. 2008; 13:1303–1321. [PubMed: 18839313]
16. Zheng Y, Ikeda K, Nakamura M, Takasaka T. Endonuclease cleavage of DNA in the aged cochlea of Mongolian gerbil. Hear Res. 1998; 126(1–2):11–18. [PubMed: 9872129]
17. Hockenbery DM, Oltvai ZN, Yin XM, Milliman CL, Korsmeyer SJ. Bcl-2 functions in an antioxidant pathway to prevent apoptosis. Cell. 1993; 75(2):241–251. [PubMed: 7503812]
18. Hosokawa M. A higher oxidative status accelerates senescence and aggravates age-dependent disorders in SAMP strains of mice. Mech Ageing Dev. 2002; 123(12):1553–1561. [PubMed: 12470893]
19. Someya S, Prolla TA. Mitochondrial oxidative damage and apoptosis in age-related hearing loss. Mech Ageing Dev. 2010; 131(7–8):480–486. [PubMed: 20434479]
20. Usami S, Takumi Y, Fujita S, Shinkawa H, Hosokawa M. Cell death in the inner ear associated with aging is apoptosis? Brain Research. 1997; 747(1):147–150. [PubMed: 9042539]
21. Deveraux QL, Leo E, Stennicke HR, Welsh K, Salvesen GS, Reed JC. Cleavage of human inhibitor of apoptosis protein XIAP results in fragments with distinct specificities for caspases. EMBO J. 1999; 18(19):5242–5251. [PubMed: 10508158]
22. Deveraux QL, Stennicke HR, Salvesen GS, Reed JC. Endogenous inhibitors of caspases. J Clin Immunol. 1999; 19(6):388–398. [PubMed: 10634212]
23. Deveraux QL, Takahashi R, Salvesen GS, Reed JC. X-linked IAP is a direct inhibitor of cell-death proteases. Nature. 1997; 388(6639):300–304. [PubMed: 9230442]
24. Liston P, Roy N, Tamai K, Lefebvre C, Baird S, Cherton-Horvat GF, et al. Suppression of apoptosis in mammalian cells by NAIP and a related family of IAP genes. Nature. 1996; 379(6563):349–353. [PubMed: 8552191]
25. Suzuki Y, Nakabayashi Y, Nakata K, Reed JC, Takahashi R. X-linked inhibitor of apoptosis protein (XIAP) inhibits caspase-3 and -7 in distinct modes. J Biol Chem. 2001; 276(29):27058–27063. [PubMed: 11359776]
26. Johnson KR, Erway LC, Cook SA, Willott JF, Zheng QY. A major gene affecting age-related hearing loss in C57BL/6J mice. Hear Res. 1997; 114(1–2):83–92. [PubMed: 9447922]
27. Syka J. Plastic changes in the central auditory system after hearing loss, restoration of function, and during learning. Physiol Rev. 2002; 82(3):601–636. [PubMed: 12087130]
28. Wang J, Tymczyszyn N, Yu Z, Yin S, Bance M, Robertson GS. Overexpression of X-linked inhibitor of apoptosis protein protects against noise-induced hearing loss in mice. Gene Ther. 2011; 18(6):560–568. [PubMed: 21228883]
29. Kujawa SG, Liberman MC. Adding insult to injury: cochlear nerve degeneration after "temporary" noise-induced hearing loss. J Neurosci. 2009; 29(45):14077–14085. [PubMed: 19906956]
30. Zilberstein Y, Liberman MC, Corfas G. Inner hair cells are not required for survival of spiral ganglion neurons in the adult cochlea. J Neurosci. 2012; 32(2):405–410. [PubMed: 22238076]
31. Wang J, Powers NL, Hofstetter P, Trautwein P, Ding D, Salvi R. Effects of selective inner hair cell loss on auditory nerve fiber threshold, tuning and spontaneous and driven discharge rate. Hear Res. 1997; 107(1–2):67–82. [PubMed: 9165348]
32. Ohlemiller KK, Gagnon PM. Apical-to-basal gradients in age-related cochlear degeneration and their relationship to "primary" loss of cochlear neurons. J Comp Neurol. 2004; 479(1):103–116. [PubMed: 15389608]

33. Thiers FA, Nadol JB Jr, Liberman MC. Reciprocal synapses between outer hair cells and their afferent terminals: evidence for a local neural network in the mammalian cochlea. J Assoc Res Otolaryngol. 2008; 9(4):477–489. [PubMed: 18688678]

34. Ruan Q, Ao H, He J, Chen Z, Yu Z, Zhang R, et al. Topographic and quantitative evaluation of gentamicin-induced damage to peripheral innervation of mouse cochleae. NeuroToxicology. 2014; 40:86–96. [PubMed: 24308912]

35. Wilson JL, Henson MM, Henson OW Jr. Course and distribution of efferent fibers in the cochlea of the mouse. Hear Res. 1991; 55:98–108. [PubMed: 1752800]

36. Schwartz AM, Parakkal M, Gulley RL. Postnatal development of spiral ganglion cells in the rat. Am J Anat. 1983; 167:33–41. [PubMed: 6869308]

37. Dau J, Wenthold RJ. Immunocytochemical localization of neurofilament subunits in the spiral ganglion of normal and neomycin-treated guinea pigs. Hear Res. 1989; 42:253–263. [PubMed: 2606806]

38. Fritzsch B. Fast axonal diffusion of 3000 molecular weight dextran amines. J Neurosci Methods. 1993; 50:95–103. [PubMed: 7506342]

39. Kobbert C, Apps R, Bechmann I, Lanciego JL, Mey J, Thanos S. Current concepts in neuroanatomical tracing. Prog Neurobiol. 2000; 62:327–351. [PubMed: 10856608]

40. Huang L, Thorne P, Houseley G, Montgometry J. Spatiotemporal definition of neurite outgrowth, refinement and retraction in the developing mouse cochlea. Development. 2007; 134:2925–2933. [PubMed: 17626062]

41. Hafidi A. Peripherin-like immunoreactivity in type II spiral ganglion cell body and projections. Brain Res. 1998; 805:181–190. [PubMed: 9733963]

42. Hafidi A, Despres G, Romand R. Ontogenesis of type II spiral ganglion neurons during development: peripherin immunohistochemistry. Int J Dev Neurosci. 1993; 11:507–512. [PubMed: 8237466]

43. Mou K, Adamson CL, Davis RL. Time-dependence and cell type specificity of synergistic neurotrophin actions on spiral ganglion neurons. J Comp Neurol. 1998; 402:129–139. [PubMed: 9831050]

44. Schimmang T, Tan J, Muller M, Zimmermann U, Rohbock K, Kopschall I, et al. Lack of Bdnf and TrkB signalling in the postnatal cochlea leads to a spatial reshaping of innervation along the tonotopic axis and hearing loss. Development. 2000; 130:4741–4750.

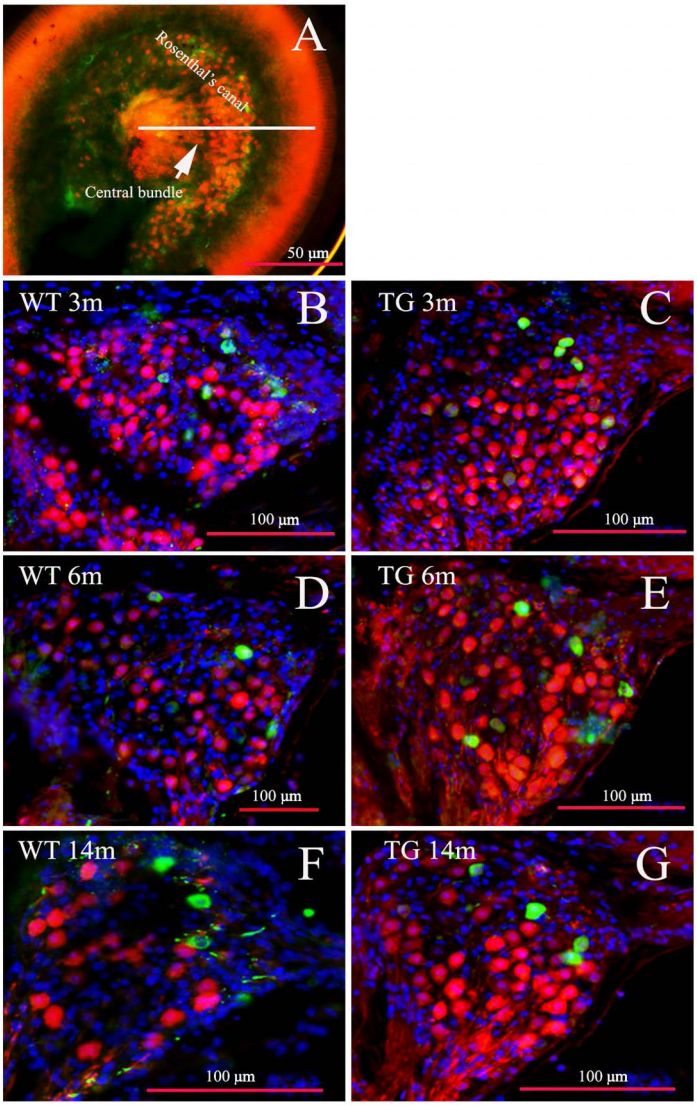

Fig. 1.

Representative images of double-stained SGNs in Rosenthal's canal in the middle turn. Type I SGNs were stained red for TMRD and type II SGNs green for peripherin. A: Overall view of whole-mount preparation. The blue spots are nuclei stained with DAPI. The white line shows the orientation of sections crossing Rosenthal's canal. Scale bars: yellow = 50 μm, red = 100 μm. B, D, F and C, E, G show images of the WT and TG groups, respectively, at the indicated ages.

Fig. 2.

Reduction of SGNs with aging. The numbers are the counts of SGNs per section view crossing Rosenthal's canal. The counts were averaged from at least 10 sections over a distance of four HP openings along the canal. The data were obtained in the M5 segment of the basilar membrane. Asterisks indicates significance: *: $P < 0.05$, **: $P < 0.01$, and ***: $P < 0.001$ ($n = 7$ in each genotype group at each age).

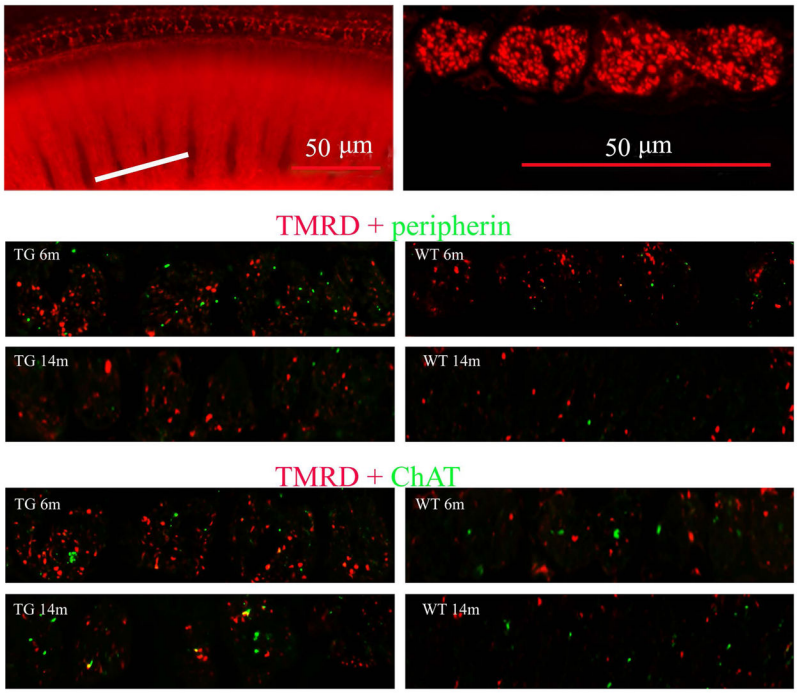

Fig. 3.

HP cross-sections at different ages stained for TMRD (for type I afferent dendrites, red) + peripherin (for type II efferent axons, green) or ChAT (for efferent axons, green) per unit length of 0.13 mm. The upper panel shows the **o**rientation of sections crossing HPs.

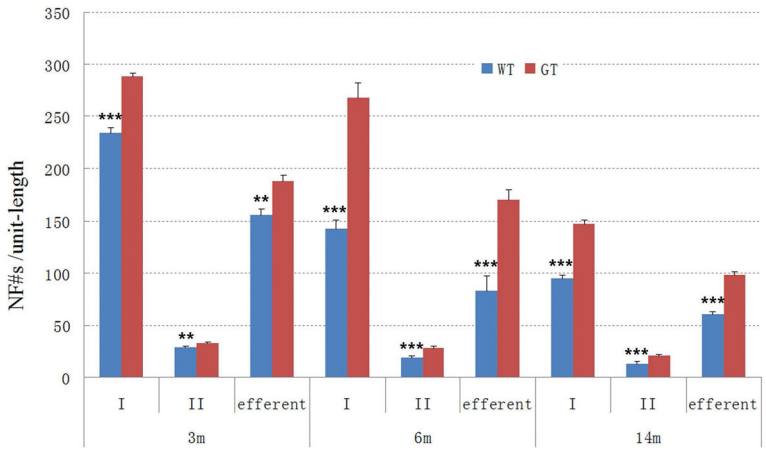

Fig. 4.

Changes in neurites as a function of age. Asterisks indicate significance: **, $P < 0.01$; ***, $P < 0.001$ ($n = 4$ each WT and TG at each age).

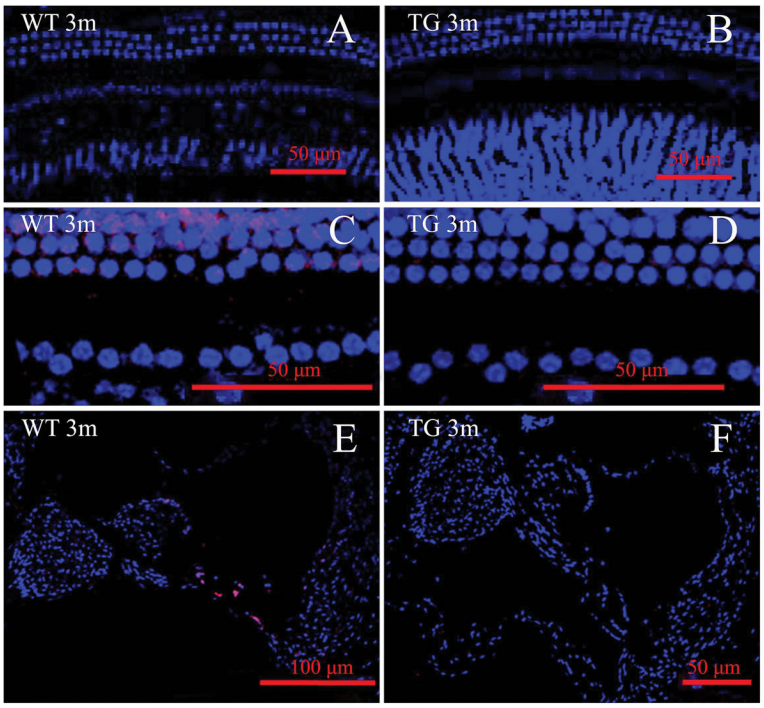

Fig. 5.

Apoptosis with aging in the cochlea. TUNEL (green) and DAPI (blue) staining were observed in the organ of Corti in M5 segments for both WT and GT mice (A – D) as well in cross-sections of Rosenthal's canal (E and F). Positive TUNEL staining was seen in both the organ of Corti and Rosenthal's canal at 6 months of age only in the WT group. The scale bar sizes are shown in the images ($n = 3$ animals in each group at each age).